Generation of a pure phase-modulated pulse by the cascading effect: a theoretical approach

L. Videau and C. Rouyer

Commissariat à l'Energie Atomique, Centre d'Etudes Scientifiques et Techniques d'Aquitaine, Boîte Postale 2, 33114 Le Barp, France

J. Garnier

Centre de Mathématiques Appliquées, Unité Mixte de Recherche 7641, Centre National de la Recherche Scientifique, Ecole Polytechnique, 91128 Palaiseau Cedex, France

A. Migus

Laboratoire pour l'Utilisation des Lasers Intenses, Unité Mixte de Recherche 7605, Centre National de la Recherche Scientifique et Commissariat à l'Energie Atomique, Ecole Polytechnique, 91128 Palaiseau Cedex, France

Received September 7, 1999; revised manuscript received February 2, 2000

New techniques to produce spatiotemporal phase modulation without the use of electro-optic devices are proposed and discussed. By using the nonlinear second-order effect in crystal it is possible to change the amplitude modulation of a pump wave into the phase of a signal wave. To that end, we propose the use of a well-known cascading configuration for which the phase mismatch is high. Analytical results of spatial and temporal incoherent phase modulation are developed with the correlation function formalisms. Furthermore, highly accurate expansions of signal phase and intensity are derived. The effects of group-velocity difference, group-velocity dispersion, and diffraction on the change of amplitude into phase modulation are studied. Finally, an experimental demonstration of a KDP crystal with a sinusoidal pump modulation that creates sinusoidal phase modulation is proposed. © 2000 Optical Society of America [S0740-3224(00)01805-1]

OCIS codes: 190.2620, 230.1150, 190.0190.

1. INTRODUCTION

The development of high-power laser chains has been studied extensively, especially for inertial confinement fusion. For the French Laser MegaJoule project[1] and for the U.S. National Ignition Facility project,[2] a major issue is uniformity of illumination of the target.[3] A direct-drive scheme requires a contrast level of less than 5% per beam, which can be obtained only with two-dimensional optical smoothing techniques[4] such as smoothing by an optical fiber[5] and two-dimensional smoothing by spectral dispersion.[6] The former technique can easily achieve this level, but with large amplitude modulation all along the laser chain. It produces nonlinear effects caused by propagation, amplification, or frequency conversion that reduce laser performance.[7] In particular, frequency-conversion efficiency drops dramatically, and the focal spot is poorly controlled at the third harmonic. Two-dimensional smoothing by spectral dispersion, however, involves fewer difficulties for the laser. In particular, the frequency-conversion efficiency is not reduced by amplitude modulation. Furthermore, the broadband spectrum is produced by a sinusoidal phase modulator with a limited bandwidth and above all with coherent phase modulation. As a result, all spatial frequencies are not smoothed by this periodic coherent phase modulation.[4]

Here we propose and analyze new smoothing techniques that involve the cascading effect. An important objective in this paper is to propose the transformation of incoherent amplitude modulation of a pump beam into the phase of a monochromatic plane-wave signal. We use nonlinear cascaded processes that create crossed phase modulation without efficient energy transfer.[8–10] With this technique we should be able to produce temporal or spatial incoherent phase modulation.

In Section 2 we describe the mechanisms that we intend to use, such as a random temporal phase modulator and a temporally varying random phase plate. In Section 3 we present theoretical results by developing analytical calculations of the nonlinear phase. In particular, we explain behavior reported by other authors. In Section 4 we present statistical results for the correlation function that take into account temporal limitations such as group-velocity dispersion (GVD) and group-velocity walk-off (GVW). Finally, in Section 5 we present a sinusoidal phase-modulator setup.

2. PHASE MODULATION BY CASCADING

A. Principles

We wish to generate pure random phase modulation with an incoherent amplitude-modulated wave. This wave is the pump wave, the phase-modulated wave is the signal wave. Throughout this paper the input signal wave is assumed to be a monochromatic plane wave. By using a

nonlinear crystal we make the two waves interact to produce a harmonic wave. Furthermore, in specific conditions the pump wave induces only nonlinear phase modulation in the signal wave.[8,9] As the crystal is far from being in a phase-matching condition, there is no frequency conversion, and the signal wave is not amplitude modulated. Figure 1 shows schematically the transformation of amplitude modulation into pure phase modulation. We call this two-wave interaction a type II configuration, because the two waves have perpendicular polarization. If the pump depletion is negligible, we have an approximate result for the nonlinear phase because of the interaction of the signal wave[11]:

$$\phi_{\mathrm{NL}}(x, y, t) = -\frac{2I_p(x, y, t)L}{\Delta k P_c}, \tag{1}$$

where L is the crystal length, I_p is the pump intensity, Δk is the phase mismatch, and

$$P_c = \frac{\epsilon_0 c n_s n_p n_h \lambda_s \lambda_p}{8\pi^2 d_{\mathrm{eff}}^2}, \tag{2}$$

where $n_{s,p,h}$ are, respectively, the signal wave, the pump wave, and the harmonic wave; λ_s is the signal wavelength and λ_p is the pump wavelength; and d_{eff} is the nonlinear coefficient. The phase is proportional to the pump intensity, so we can consider the two-wave interaction to be a nonlinear Kerr effect[12] for a signal wave characterized by the nonlinear coefficient $n_2 = 2/k_0 \Delta k P_c$. At the output of the crystal, the signal wave has a modulated phase that is proportional to the pump amplitude modulation, whereas its amplitude is not changed. With this method we can generate an incoherent phase modulator in the temporal domain, an incoherent phase plate in the spatial domain, or a time-varying phase plate in the spatiotemporal domain. In fact, this method is the same as that of cross modulation but it is an extension into the spatial domain with a nonlinear technique that permits many configurations to exist and is certainly more efficient. To study the statistical properties of the signal wave, we introduce in Subsection 2.B the correlation functions of the pump and the signal waves.

B. Statistical Characteristics of the Incoherent Phase Modulator, the Incoherent Phase Plate, and the Time-Varying Phase Plate

In fact, the results for the three phase-plate schemes are the same in terms of statistical calculations. So all the results obtained for the temporal domain are valid for the spatial domain. In what follows, we use the temporal variable, but this is an arbitrary choice. In this way we assume that the pump wave is a partially coherent pulse characterized by its correlation function $f_p(t) = I_p{}^{-1}\langle E_p(0)E_p^*(t)\rangle$, where I_p is the average intensity $\langle E_p E_p^*\rangle$. By the Wiener–Khintchine theorem[13] we can deduce the spectral intensity $\tilde{I}_p(\nu)$ of the pump from the Fourier transform of $f_p(t)$:

$$\tilde{I}_p(\nu) = \int_{-\infty}^{+\infty} f_p(t)\exp(-2i\pi\nu t)\mathrm{d}t. \tag{3}$$

For example, we may assume a Gaussian-type correlation function for the pump field:

$$f_p(t) = \frac{1}{I_p}\langle E_p(0)E_p^*(t)\rangle = \exp(-t^2/2t_c^2), \tag{4}$$

$$\tilde{I}_p(\nu) = \tilde{I}_p \exp(-\nu^2/2\nu_c^2), \tag{5}$$

where t_c is the coherence time and ν_c is the spectral bandwidth equal to $(2\pi t_c)^{-1}$. Using Eq. (1) for the nonlinear phase and assuming that the signal amplitude is equal to 1, we find that the correlation function of the signal wave is[14]

$$f_s(t) = \frac{1}{1 + B(L)^2[1 - f_p^2(t)]}, \tag{6}$$

where $B(L)$ is the positive averaged phase:

$$B(L) = \frac{2I_p L}{\Delta k P_c}. \tag{7}$$

With a simple Fourier transform, we also have the spectral intensity of the signal wave, which has two parts, a Dirac function and a continuous function, whose respective weights are $\alpha = [1 + B(L)^2]^{-1}$ and $(1 - \alpha)$:

$$\begin{aligned}\tilde{I}_s(\nu) &= \int_{-\infty}^{+\infty} f_s(t)\exp(-2i\pi\nu t)\mathrm{d}t \\ &= \alpha\delta(\nu) + (1 - \alpha)\tilde{\tilde{I}}_s^c(\nu),\end{aligned} \tag{8}$$

with

$$\tilde{\tilde{I}}_s^c(\nu) = \int_{-\infty}^{+\infty} \frac{f_p^2(t)}{1 + B(L)^2[1 - f_p^2(t)]}\exp(-2i\pi\nu t)\mathrm{d}t. \tag{9}$$

We have plotted in Fig. 2 the correlation functions and the spectral intensity of the signal wave for $B = 1$ and $B = 2$. We have also plotted the input functions as references. We can see that the signal spectrum width is larger than that of the pump, even for $B = 1$. By this technique, we can generate an incoherent phase modulator and control its characteristics by choosing an efficient correlation function shape and a suitably averaged phase $B(L)$.

As we said above, these results are available in the spatial domain. We have only to replace temporal variable (t) by spatial transverse variables (x, y) and the coherence time by the correlation radius. If we focus the wave through a lens, we obtain a focal spot that is a speckle pattern[15] as a result of phase interferences. The envelope of the spot is exactly the spectral intensity of the signal wave, and its correlation radius (different from that of the signal wave) is defined only by the focal length and

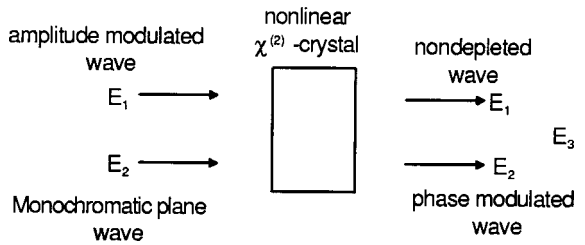

Fig. 1. Schematic of the setup for the conversion of amplitude modulation into phase modulation.

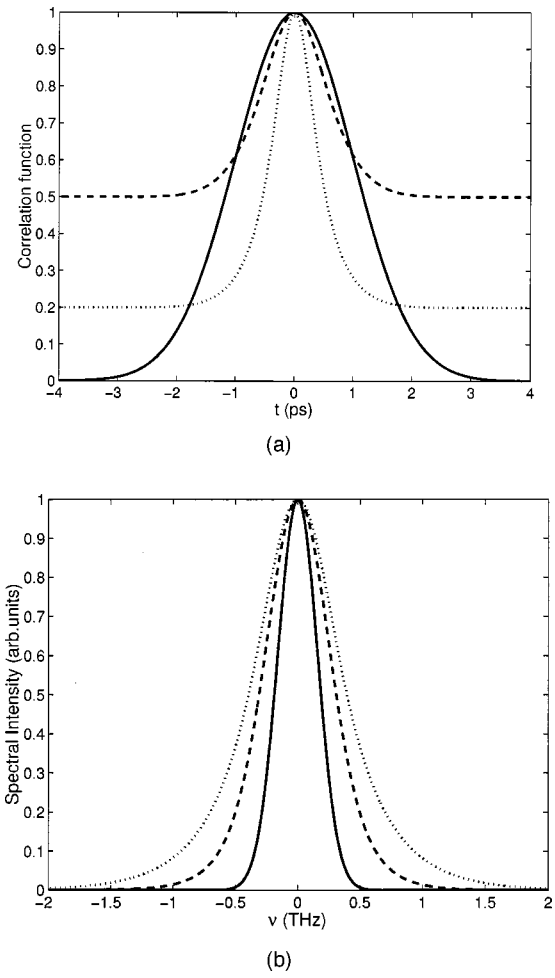

Fig. 2. (a) Correlation function and (b) spectral intensity for the signal and the pump waves. Solid curves, pump functions; dashed curves, signal wave for $B = 1$; dotted curves, signal wave for $B = 2$. The pump correlation function is a Gaussian function with a coherence time t_c of 1 ps. We removed the Dirac function from the spectra.

the geometry of the whole beam. A limit of the system appears here in the control of the focal spot's shape.

For the time-varying phase plate we have a signal wave with temporal and spatial modulation. We can consider that the generated phase plate is moving during the laser coherence time; the correlation function should be generalized with (t) replaced by (x, y, t).

After this description of the three kinds of phase modulator with the cascading effect, we now develop calculations for nonlinear phase and amplitude modulation for the signal wave.

3. THEORETICAL RESULTS IN THE CASCADING CONFIGURATION

In Section 2 we used a phase expression [Eq. (1)] that we obtained by neglecting pump depletion and cubic nonlinearity. In this section we take into account the complete system of frequency-conversion equations and develop analytical results for a small parameter γ^{-1} defined with crystal and laser parameters that characterizes the phase mismatch (the smaller γ^{-1}, the larger the phase mismatch). We continue to neglect the effects of cubic nonlinearity because we assume here that it has an insignificant influence on nonlinear phase modulation.

A. Derivation of the Main Results

Frequency conversion entails three coupled equations, for signal wave E_s, pump wave E_p, and harmonic wave E_h. We normalized the equations such that intensity I_j is simply the square modulus of E_j. Electric field $\mathcal{E}_j$ is then given by

$$\mathcal{E}_j = \left[\frac{1}{2n(\omega_j)c\epsilon_0}\right]^{1/2} E_j \exp i(k_j z - \omega_j t) + \text{c.c.} \quad (10)$$

In this section we assume that the waves follow the frequency-conversion equations for monochromatic plane waves. In particular, we remove temporal or diffraction effects. Then the normalized fields can be described by the following system of equations[16]:

$$\frac{\partial E_s}{\partial z} = i\sqrt{\frac{\omega_s}{\omega_p}}\frac{1}{\sqrt{P_c}} E_p^* E_h \exp(i\Delta k z),$$

$$\frac{\partial E_p}{\partial z} = i\sqrt{\frac{\omega_p}{\omega_s}}\frac{1}{\sqrt{P_c}} E_s^* E_h \exp(i\Delta k z),$$

$$\frac{\partial E_h}{\partial z} = i\frac{\omega_h}{\sqrt{\omega_p\omega_s}}\frac{1}{\sqrt{P_c}} E_p E_s \exp(-i\Delta k z), \quad (11)$$

where ω_j are the frequencies of the waves, Δk is the phase mismatch, and P_c is given by Eq. (2). We can solve these equations and obtain analytical results for the phase and the amplitudes of the three waves. We focus here on the case without an initial harmonic wave, and the results are given in Appendix A. We expanded the intensity and the phase up to the third order of γ^{-1}, where $\gamma = P_c\Delta k^2/I_t$ and I_t is the sum of the three intensities. It is interesting to consider expansion to first order of the phase and the intensity, assuming that the input phases are null. We put $E_j = \sqrt{I_j}\exp i\phi_j$ and find that

$$I_{s,p}(z) = I_{s0,p0} - \frac{8I_{s0}I_{p0}}{P_c\Delta k^2}\sin^2[\phi(z)], \quad (12)$$

$$\phi_{s,p}(z) = -\frac{2I_{p0,s0}}{P_c\Delta k^2}\{\Delta k z - \sin[2\phi(z)]\}, \quad (13)$$

where $\phi(z)$ is given by Eq. (A8) below and can be expanded at first order as $\phi(z) = (\Delta k z/2)(1 + 4\gamma^{-1})$. These calculations are valid for a type II configuration with two waves, a signal wave and a pump wave. Therefore we have similar expressions if we have a single wave at the input. In this case, we assume that the input wave has an intensity I_i. Then we merely have to rewrite Eqs. (12) and (13), taking into account that $I_s = I_p = I_i/2$, and $I_t = I_i$. We find the following expansions for this type I configuration (one input wave):

$$I_i(z) = I_i - \frac{4I_i^2}{P_c\Delta k^2}\sin^2[\,\phi(z)], \tag{14}$$

$$\phi_i(z) = -\frac{I_i}{P_c\Delta k^2}\{\Delta kz - \sin[2\phi(z)]\}. \tag{15}$$

B. Comparison of Expansions and Analytical Results

With these formulas we can retrieve numerical results when the parameter γ^{-1} is small. For instance, we studied a type I configuration in which the pump and the signal waves have equal intensities. In the case corresponding to Fig. 3, we have $\gamma = 36$ and a maximum nonlinear phase of 0.7 rad. The solid curves are the reference curves that we obtained with a numerical code that solved the system of Eqs. (11), whereas the dotted curves correspond to the first-order calculation and the dashed curves correspond to the second-order calculation. The behavior of the phase is well known, with a sinusoidal part in addition to a linear slope.[8,11] But the first-order expansion of the phase predicts this behavior with good accuracy. Furthermore, it would be relevant to use the second-order expansion (see Appendix A) for devices that require the nonlinear phase to be produced with high precision.

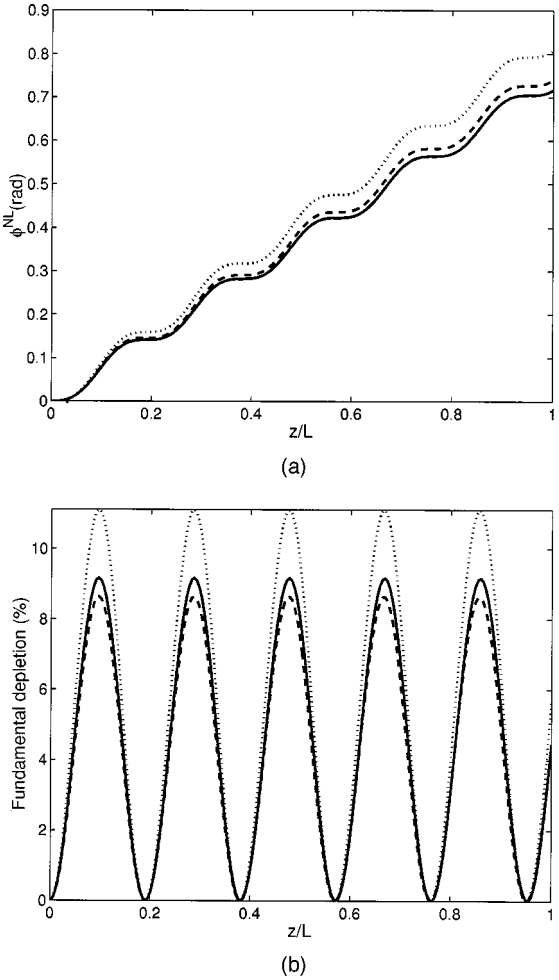

Fig. 3. (a) Nonlinear phase and (b) intensity depletion as functions of the ratio z/L in a type I configuration. Solid curves, numerical results; dotted curves, obtained with a first-order expansion; dashed curves, obtained with a second-order expansion. $L = 1$ cm, $I = 25\ \mathrm{GW/cm^2}$, $P_c = 1$ GW, $\Delta k = 30\ \mathrm{cm^{-1}}$.

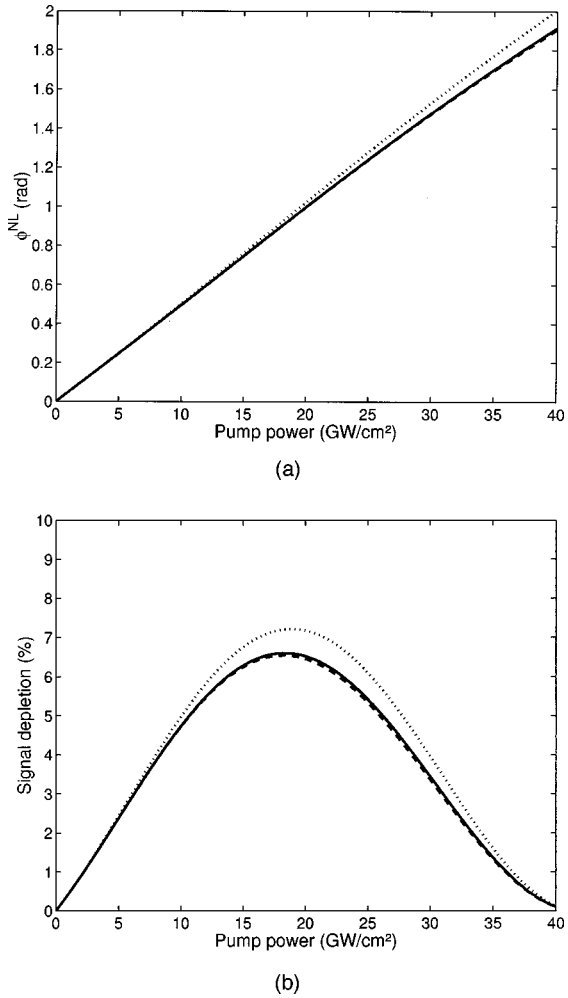

Fig. 4. (a) Nonlinear phase and (b) intensity depletion of the signal wave as functions of the pump intensity in a type II configuration. Solid curves, numerical results; dotted curves, obtained with a first-order expansion; dashed curves, obtained with a second-order expansion. $L = 1$ cm, $I_{s0} = 0.1\ \mathrm{GW/cm^2}$, $P_c = 1$ GW, $\Delta k = 40\ \mathrm{cm^{-1}}$.

We also studied a type II configuration. In Fig. 4 the signal wave has an intensity that is much lower than that of the pump wave, and the nonlinear phase and the signal depletion are plotted as functions of the pump intensity. For the maximum plotted pump intensity, the parameter γ is equal to 40. The second-order results are similar to the numerical results, whereas there is a small difference when we use only the first-order expansion. So we have good agreement between expansions and numerical results. The nonlinear phase is then almost proportional to the pump intensity that is required for the three configurations that we proposed in Section 2. The resultant amplitude modulations here are less than 6% for the signal wave. So we have a good prediction of the nonlinear phase and the signal depletion that will be produced. We have shown that in certain conditions the nonlinear phase is linearly dependent on the pump intensity, which was our assumption in Section 2. γ^{-1} is consequently a relevant parameter with which to verify this assumption.

4. ESTIMATIONS OF DIFFERENT LIMITATIONS

In Section 2 we described the correlation function of the signal wave. We assumed that the frequency-conversion equations for monochromatic waves were valid in our configurations. In fact, such is not true if the coherence time is of the order of several picoseconds. We now study the effects of temporal limitations. In Subsection 4.A we take into account the GVW and in Subsection 4.B we deal with the GVD. Indeed, in Subsection 4.C we show similar results in spatial domain.

A. Group-Velocity Walk-Off

The system of coupled equations for the three interacting waves is not the same as Eqs. (11) if we take into account GVW. It must be changed into the following system, which is written in the pump moving-time pulse frame[17]:

$$\frac{\partial E_s}{\partial z} = -\Delta_s^v \frac{\partial E_s}{\partial t} + i\sqrt{\frac{\omega_s}{\omega_p}}\frac{1}{\sqrt{P_c}} E_p^* E_h \exp(i\Delta k z),$$

$$\frac{\partial E_p}{\partial z} = i\sqrt{\frac{\omega_p}{\omega_s}}\frac{1}{\sqrt{P_c}} E_s^* E_h \exp(i\Delta k z),$$

$$\frac{\partial E_h}{\partial z} = -\Delta_h^v \frac{\partial E_h}{\partial t} + i\frac{\omega_h}{\sqrt{\omega_p \omega_s}}\frac{1}{\sqrt{P_c}} E_p E_s \exp(-i\Delta k z), \quad (16)$$

where $\Delta_s^v = (v_s^g)^{-1} - (v_p^g)^{-1}$ and $\Delta_h^v = (v_h^g)^{-1} - (v_p^g)^{-1}$, with $(v^g)^{-1} = \partial k/\partial\omega$. When the phase mismatch and the pump intensity are strong enough, we can apply the homogenization theorem (see Appendix B), which establishes that the pump wave is unperturbed and that the signal wave follows the effective equation

$$\frac{\partial E_s(z,t)}{\partial z} = -\Delta_s^v \frac{\partial E_s(z,t)}{\partial t} - i\frac{2I_p(z,t)}{\Delta k P_c} E_s(z,t), \quad (17)$$

whose solution is $E_s(z,t) = \exp i\phi(z,t)$, with

$$\phi(z,t) = -\frac{2}{\Delta k P_c}\int_0^z I_p(t - \Delta_s^v z')\mathrm{d}z'. \quad (18)$$

Note that the harmonic group-velocity difference does not appear in the effective equation for the signal wave. The signal amplitude is unperturbed; there is only a phase average. It is not possible to derive a closed-form expression for the signal correlation function from Eq. (18). Nevertheless, we can expand the expression with respect to $\Delta_s^v z t_c^{-1} \ll 1$ and find that

$$f_s(t) = f_{s0}(t)\left\{1 + \frac{\Delta_s^{v2} z^2}{6t_c^2} B(z)^2 f_{s0}^2[g_1(t/t_c) + B(z)^2 g_2(t/tc)]\right\} + O\left[\left(\frac{\Delta_s^v z}{t_c}\right)^3\right], \quad (19)$$

where f_{s0} is the signal correlation function without GVW [Eq. (6)] and $\tilde{f}_p$ is the normalized correlation function of the pump field:

$$\tilde{f}_p(u) = f_p(u t_c),$$

$$g_1(u) = -\tilde{f}_p''(0) + \tilde{f}_p'^2(u) + \tilde{f}_p\tilde{f}_p''(u),$$

$$g_2(u) = \tilde{f}_p''(0)[\tilde{f}_p^2(u) - 1] + \tilde{f}_p'^2(u) + \tilde{f}_p\tilde{f}_p''(u) + 3\tilde{f}_p^2\tilde{f}_p'^2(u) - \tilde{f}_p^3\tilde{f}_p''(u).$$

The expression for the spectral intensity is the same as Eq. (8); the parameter α is now

$$\tilde{I}_s(\nu) = \int_{-\infty}^{+\infty} f_s(t)\exp(-2i\pi\nu t)\mathrm{d}t = \alpha\delta(\nu) + (1-\alpha)\tilde{I}_s^c(\nu),$$

$$\alpha = \frac{1}{1 + B(L)^2}\left[1 - \frac{\Delta_s^{v2} L^2}{6t_c^2}\frac{B(L)^2}{1 + B(L)^2}\tilde{f}_p''(0)\right]. \quad (20)$$

Because $\tilde{f}_p''(0)$ is always negative [$\tilde{f}_p(0)$ is a maximum point], the continuous contribution to the signal spectral intensity is reduced compared with that of the Dirac function. So the effects of the GVW are a spectral narrowing and a broadening of the correlation function. For example, we studied this effect with case $B = 2$ as shown in Fig. 2 by adding a nonzero group-velocity difference. We have plotted in Fig. 5 the case when $B^2\Delta_s^{v2} z^2/6t_c^2 = 0.2$. We can notice the broadening of the correlation function, whereas the spectral intensity is narrower. In fact, the main perturbation in the spectrum is on the wings, which decrease quickly. Indeed, the phase average that is due to the group-velocity difference in Eq. (18) is more important for high frequencies than for low frequencies.

B. Effects of Group-Velocity Dispersion

For short coherence times (a few picoseconds), another main temporal limitation is the GVD. The system of Eqs. (11) then can be written as

$$\frac{\partial E_s}{\partial z} = -i\sigma_s\frac{\partial^2 E_s}{\partial t^2} + i\sqrt{\frac{\omega_s}{\omega_p}}\frac{1}{\sqrt{P_c}} E_p^* E_h \exp(i\Delta k z),$$

$$\frac{\partial E_p}{\partial z} = -i\sigma_p\frac{\partial^2 E_p}{\partial t^2} + i\sqrt{\frac{\omega_p}{\omega_s}}\frac{1}{\sqrt{P_c}} E_s^* E_h \exp(i\Delta k z),$$

$$\frac{\partial E_h}{\partial z} = -i\sigma_h\frac{\partial^2 E_h}{\partial t^2} + i\frac{\omega_h}{\sqrt{\omega_p \omega_s}}\frac{1}{\sqrt{P_c}} E_p E_s \exp(-i\Delta k z), \quad (21)$$

where $\sigma_i = [k''(\omega_i)/2]$. Applying the homogenization theorem, we find that E_s follows a new effective equation:

$$\frac{\partial E_s(z,t)}{\partial z} = -i\sigma_s\frac{\partial^2 E_s(z,t)}{\partial t^2} - i\frac{2I_p(z,t)}{\Delta k P_c} E_s(z,t), \quad (22)$$

which shows that only the signal GVD has to be taken into account. We cannot find a closed equation for E_s, but we can expand solutions for a small GVD effect ($|\sigma_s z/t_c^2| \ll 1$). Then the correlation function of the signal wave is given by the following relation:

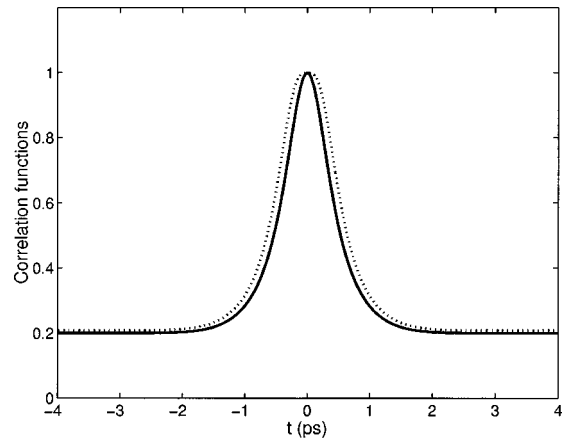

(a)

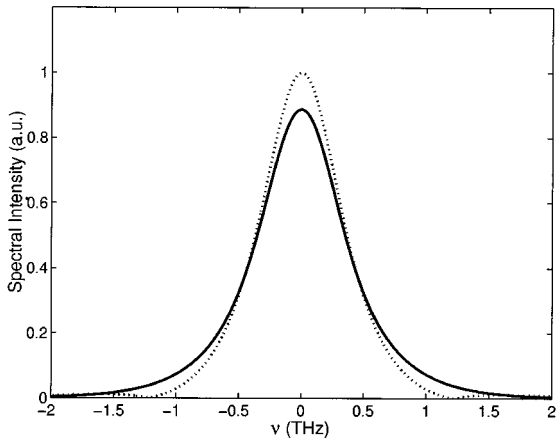

(b)

Fig. 5. (a) Correlation function and (b) spectral intensity for the signal wave in the same configuration as Fig. 2. Solid curves, without the group-velocity difference effect; dotted curves, $B^2\Delta_s^{v2}z^2/6t_c^2 = 0.2$.

$$f_s(t) = f_{s0}(t)\left\{1 - \frac{2\sigma_s L}{3t_c^2}B(L)^3\tilde{f}_p''(0)[1 - \tilde{f}_p(t/t_c)^2]f_{s0}(t)\right\} + O\left[\left(\frac{\sigma_s L}{t_c^2}\right)^2\right]. \quad (23)$$

Weight α of the Dirac function in the spectral intensity is then equal to

$$\alpha = \frac{1}{1 + B(L)^2}\left[1 - \frac{2\sigma_s L}{3t_c^2}\frac{B(L)^3}{1 + B(L)^2}\tilde{f}_p''(0)\right]. \quad (24)$$

If $\sigma_s > 0$ (normally dispersive media), the correlation function is larger and the spectral intensity is narrower. However, when $\sigma_s < 0$ (anomalous dispersive media), the spectrum is broadened and the correlation function is narrowed. These effects are enhanced by the B parameter because of the factor $B^3/(1 + B^2)$, which is growing. Furthermore, the GVD produces amplitude modulations in addition to the phase modulations. Because the correlation function at point $t = 0$ is unchanged, the average intensity is the same. These amplitude modulations are characterized by contrast $C_s(L)$ of the signal wave, defined by the identity

$$C_s^2(L) = \frac{\langle|E_s|^4\rangle - \langle|E_s|^2\rangle^2}{\langle|E_s|^2\rangle^2}. \quad (25)$$

We find the following expansion for this parameter:

$$C_s(L) = B(L)\frac{|\sigma_s|L}{t_c^2}[3/2\tilde{f}_p''(0)^2 + 2\tilde{f}^{(4)}(0)]^{1/2} + O\left[\left(\frac{\sigma_s L}{t_c^2}\right)^2\right]. \quad (26)$$

C. Spatial Limitations

All the results obtained above could be used in this section for the spatial limitations, such as angular walk-off and diffraction, that may be encountered. The angular walk-off is similar to the GVW; the diffraction, to the GVD. In this subsection we simply have to define the spatial correlation function $f_p(x, y)$:

$$f_p(x) = \frac{1}{I_p}\langle E_p(0,0)E_p^*(x, y)\rangle = \exp[-(x^2 + y^2)/2r_c^2], \quad (27)$$

where r_c is so-called the correlation radius.

1. *Effects of Angular Walk-Off*

Taking angular walk-off into account, we can rewrite the system of Eqs. (11) as

$$\frac{\partial E_s}{\partial z} = -\Delta_s^x\frac{\partial E_s}{\partial x} + i\sqrt{\frac{\omega_s}{\omega_p}}\frac{1}{\sqrt{P_c}}E_p^*E_h\exp(i\Delta kz),$$

$$\frac{\partial E_p}{\partial z} = i\sqrt{\frac{\omega_p}{\omega_s}} - \frac{1}{\sqrt{P_c}}E_s^*E_h\exp(i\Delta kz),$$

$$\frac{\partial E_h}{\partial z} = -\Delta_h^x\frac{\partial E_h}{\partial x} + i\frac{\omega_h}{\sqrt{\omega_p\omega_s}}\frac{1}{\sqrt{P_c}}E_pE_s\exp(-i\Delta kz), \quad (28)$$

where $\Delta_s^x = \tan(\alpha_p) - \tan(\alpha_s)$, $\Delta_h^x = \tan(\alpha_p) - \tan(\alpha_h)$, and α_i is the angular departure for the corresponding wave between the directions of the Poynting vector and the wave vector. Equations (28) are the same as Eqs. (16) if we replace x by t and Δ_i^x by Δ_i^v. Then the results derived in Subsection 4.A can be applied in the spatial domain to the spatial correlation function and the spatial spectral intensity.

2. *Effects of Diffraction*

When the beam divergence is so large that the corresponding Rayleigh distance is smaller than the crystal thickness, we have to take into account diffraction inside the nonlinear crystal. Then Eqs. (11) are written as

$$\frac{\partial E_s}{\partial z} = -i\sigma_s^{\mathrm{dif}}\left(\frac{\partial^2 E_s}{\partial x^2} + \frac{\partial^2 E_s}{\partial y^2}\right) + i\sqrt{\frac{\omega_s}{\omega_p}}\frac{1}{\sqrt{P_c}}E_p^*E_h\exp(i\Delta kz), \quad (29a)$$

$$\frac{\partial E_p}{\partial z} = -i\sigma_p^{\mathrm{dif}}\left(\frac{\partial^2 E_p}{\partial x^2} + \frac{\partial^2 E_p}{\partial y^2}\right) + i\sqrt{\frac{\omega_p}{\omega_s}}\frac{1}{\sqrt{P_c}}E_s^* E_h \exp(i\Delta k z), \tag{29b}$$

$$\frac{\partial E_h}{\partial z} = -i\sigma_h^{\mathrm{dif}}\left(\frac{\partial^2 E_h}{\partial x^2} + \frac{\partial^2 E_h}{\partial y^2}\right) + i\frac{\omega_h}{\sqrt{\omega_p\omega_s}}\frac{1}{\sqrt{P_c}}E_p E_s \exp(-i\Delta k z), \tag{29c}$$

where $\sigma_i^{\mathrm{dif}} = 1/(2k_i\cos^2\alpha_i)$. The system of Eqs. (29a), (29b), and (29c) is then similar to that of Eqs. (21), and the results obtained in Subsection 4.B can be applied to the spatial domain. We have only to use the spatial correlation function and to substitute σ_i for the corresponding parameter σ_i^{dif}, (∂t^2) for $(\partial x^2 + \partial y^2)$, (∂t^4) for $(\partial x^4 + 2\partial x^2 y^2 + \partial y^4)$, and t_c for r_c.

5. SINUSOIDAL PHASE-MODULATOR SETUP

In Sections 2 and 4 we assumed that the pump wave was partially coherent. Here we develop some results for a pump wave with a sinusoidal intensity behavior. The pump field is given by

$$E_p(t) = \sqrt{2I_p}\cos(2\pi\nu_m t), \tag{30}$$

so the time-averaged intensity is I_p, where ν_m is the frequency modulation. This modulated wave can be produced by a laser with two frequencies, ν_1 and ν_2, with $\nu_m = \nu_2 - \nu_1$. By using Eq. (1) we can then generate a sinusoidal phase modulation on the signal wave, where the modulation depth is equal to the factor $B_0(L)$ given by Eq. (7). The frequency modulation of the phase is $2\nu_m$:

$$E_s(t) = \exp i[B_0(L)\cos(4\pi\nu_m t)]. \tag{31}$$

We can estimate the effect of GVW by using Eq. (18). In fact, the integration is now analytical because the pump intensity has a simple sinusoidal behavior. We find that the signal phase is always sinusoidal, with the same frequency but with a different modulation depth $B(L)$:

$$B(L) = B_0(L)\mathrm{sinc}(2\pi\nu_m\Delta_s^v L), \tag{32}$$

where $\mathrm{sinc}(r) = \sin(r)/r$. This relation is an analytical result without expansion. If the GVW is too high, the depth modulation is then strongly reduced. So we have to limit the crystal depth to the value $0.1(\nu_m\Delta_s^v)^{-1}$ to obtain more than 90% of the maximum value of $B_0(L)$. Finally, we find the expression for the amplitude modulations that are due to the GVD of the signal wave:

$$C_s(L) = 4\pi^2 B(L)|\sigma_s| L\nu_m^2 + O[(4\pi^2\sigma_s L\nu_m^2)^2]. \tag{33}$$

Here $C_s(L)$ is defined as in Eq. (25), where $\langle\ \rangle$ stands for averaging over a time period. In Fig. 6 we have plotted an example of a sinusoidal phase-modulator setup with a 2-cm type II KDP crystal. The pump intensity is sinusoidal, with a frequency modulation of 10 GHz and an average intensity of 2.5 GW/cm^2. We assume here that the phase mismatch in the crystal is $\Delta k = 19.3\,\mathrm{cm}^{-1}$ and that $P_c = 1$ GW. Using Eqs. (12) and (13), we find that the maximum nonlinear phase ϕ_{NL} is 1.03 rad and the total amplitude modulation $\alpha = 2(I_{\max} - I_{\min})/(I_{\max} + I_{\min})$ is 0.11. The numerical results in Fig. 6 give $\phi_{\mathrm{NL}} = 0.95$ rad and $\alpha = 0.094$, which are extremely close to the analytical results. We omit the spatial dimension in this configuration. We have taken into account the effects of GVW and GVD, but here they appear to be negligible. No optical damage is expected in the nanosecond regime for the KDP crystal. We also estimated the cubic nonlinear phase shift, which is less than 0.1 rad for the maximal intensity.

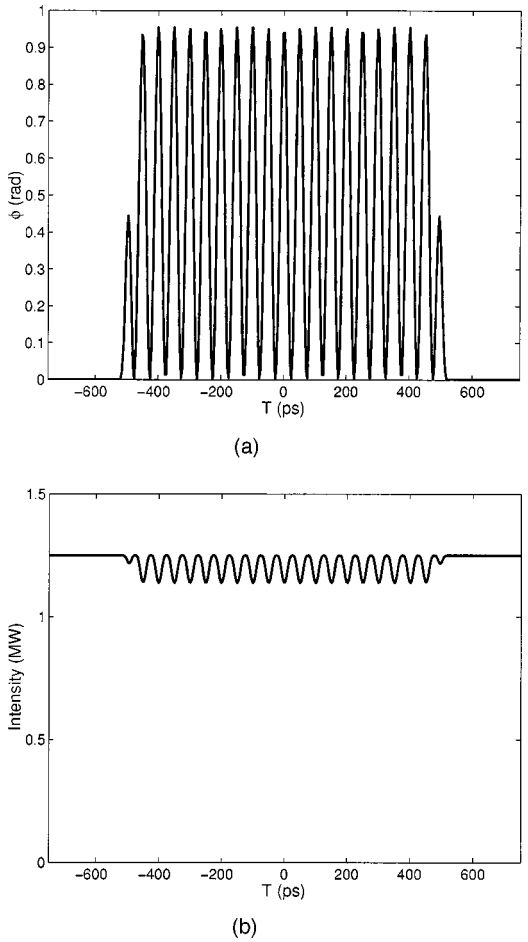

Fig. 6. (a) Nonlinear phase and (b) normalized signal intensity as a function of time (in picoseconds). The pump intensity is sinusoidal, with $\upsilon_m = 10$ GHz and $I_p = 2.5$ GW/cm^2. The crystal is assumed to be a 2-cm KDP crystal in a type II configuration. $L = 2$ cm, $P_c = 1$ GW, $\Delta k = 19.3\,\mathrm{cm}^{-1}$, $\sigma_s = -0.03$ ps^2/m.

6. CONCLUSIONS

In this paper we have described a new method for realizing a phase modulator in the spatial or the temporal domain by using a cascaded nonlinear second-order effect. We can produce a temporally incoherent phase modulator with a short coherence time or a time-varying phase plate. Furthermore, we have expanded the frequency

conversion equations to find new expressions for the signal's phase and intensity. A comparison of numerical and analytical results has shown that they are in good agreement. We have also taken into account several limitations in the temporal and spatial domains. Indeed, we have proposed a demonstration of this technique by using a bimodal laser mixed with the signal wave into a 2-cm KDP crystal. We expect a total amplitude modulation of 1 rad in this configuration, with less than 10% amplitude modulation. This technique should be interesting for two-dimensional smoothing by spectral dispersion, for which a bulk modulator with high-frequency modulation is needed. Furthermore, we can produce a time-varying phase plate by using an incoherent pump produced by a multimode optical fiber. So the signal wave should have no amplitude modulation, a condition that is important for amplification in glass amplifiers and in the frequency-conversion stage for future mega joule lasers.

APPENDIX A: HIGH-ORDER EXPRESSIONS FOR PHASES AND AMPLITUDES

Using the system described by Eqs. (11), we find the following expressions for the intensities and the phases of the three waves[18,19]:

$$
\begin{aligned}
I_{s,p}(z) &= \left\{ N_{s0,p0} - N_b \,\mathrm{sn}^2\left[\left(\frac{N_c I_t}{P_c} \right)^{1/2} m \right] \right\} \frac{\omega_{s,p}}{\omega_h} I_t ,\\
I_h(z) &= N_b \,\mathrm{sn}^2\left[z \left(\frac{N_c I_t}{P_c} \right)^{1/2} z,\, m \right] I_t ,\\
\phi_{s,p} &= \phi_{s0,p0} + \frac{1}{2}\Delta k z - \left(\frac{P_c}{I_t N_c} \right)^{1/2} \frac{\Delta k}{2} \\
&\quad \times \prod \left\{ \frac{N_b}{N_{s0,p0}},\, \mathrm{am}\left[z \left(\frac{N_c I_t}{P_c} \right)^{1/2} m \right],\, m \right\},\\
\phi_h &= \phi_{s0} + \phi_{p0} + \frac{\pi}{2}\Delta k z,
\end{aligned}
\tag{A1}
$$

where $I_t = I_{s0} + I_{p0}$, ϕ_{j0} is the input phase, I_{j0} is the input intensity, $N_{j0} = (\omega_h I_{j0})/(\omega_j I_t)$, and N_b and N_c are the two solutions of the following second-degree equation ($N_b \leqslant N_c$):

$$
N^2 - \left(N_{s0} + N_{p0} + \frac{1}{4}\frac{P_c}{I_t}\Delta k^2 \right) N + N_{s0} N_{p0} = 0, \tag{A2}
$$

where m is the ratio N_b/N_c. The functions sn and am are, respectively, the Jacobian function and the amplitude function, defined by[20]

$$
\begin{aligned}
\mathrm{sn}^{-1}(x,\, m) &= \int_0^x \frac{\mathrm{d}t}{[(1 - t^2)(1 - m t^2)]^{1/2}},\\
\mathrm{am}(u,\, m) &= \arcsin[\mathrm{sn}(u,\, m)].
\end{aligned}
\tag{A3}
$$

The symbol Π refers to an integral of the third kind, defined by the expression[20]

$$
\prod (n,\, \phi,\, m) = \int_0^{\phi} \frac{\mathrm{d}\theta}{(1 - n \sin^2\theta)[(1 - m \sin^2\theta)]^{1/2}}. \tag{A4}
$$

For further calculations we introduce two parameters, $\beta = N_{p0} N_{s0} (\beta \leqslant 1)$ and $\gamma = P_c \Delta k^2 / I_t$. In a cascading configuration, we assume that $\gamma^{-1} \ll 1$. Furthermore, we assume that the signal and the pump waves have the same frequency, such that $N_{10} + N_{20} = 2$. Under these assumptions, we can expand all parameters with respect to γ^{-1}:

$$
\begin{aligned}
N_c &= \frac{\gamma}{4} + 2 - \frac{4\beta}{\gamma}\left(1 - \frac{8}{\gamma} \right) - \frac{64\beta}{\gamma^3}(\beta + 4) \\
&\quad + \frac{512\beta}{\gamma^4}(3\beta + 4),
\end{aligned}
\tag{A5}
$$

$$
N_b = \frac{4\beta}{\gamma}\left(1 - \frac{8}{\gamma} \right) + \frac{64\beta}{\gamma^3}(\beta + 4) - \frac{512\beta}{\gamma^4}(3\beta + 4), \tag{A6}
$$

$$
m = \frac{16\beta}{\gamma^2}\left(1 - \frac{16}{\gamma} \right) + \frac{512\beta}{\gamma^4}(6 + \beta), \tag{A7}
$$

$$
\begin{aligned}
\phi(z) = z\left(\frac{N_c I_t}{P_c} \right)^{1/2} &= \frac{\Delta k z}{2}\left[1 + \frac{4}{\gamma} - \frac{8}{\gamma^2}(1 + \beta) \right. \\
&\quad \left. + \frac{32}{\gamma^3}(1 + 3\beta) - \frac{160}{\gamma^4}(1 + 6\beta + \beta^2) \right].
\end{aligned}
\tag{A8}
$$

Now we can use expansions of the Jacobian function and the third kind of integral[21]:

$$
\begin{aligned}
\mathrm{sn}(u,\, m) &= \sin(u) - {}^1\!/_4 m[u - {}^1\!/_2 \sin(2u)] \\
&\quad \times \cos(u) + O(m^2),
\end{aligned}
\tag{A9}
$$

$$
\prod (n,\, \phi,\, m) = \sum_{l=0}^{+\infty} \sum_{j=0}^{l} n^l (-1)^j t_{2l}(\phi) \binom{-1/2}{j} \left(\frac{m}{n} \right)^j , \tag{A10}
$$

with $t_{2l}(\phi) = (2l - 1/2l) t_{2(l-1)}(\phi) - (1/2l)\sin^{(2l-1)}(\phi) \times \cos(\phi)$ and $t_0(\phi) = \phi$. $\binom{a}{n} = a(a-1)\ldots(a-n+1)/1, 2, 3 \ldots n$, and $\binom{a}{0} = 1$. Finally, we obtain the following expressions for the phase and the amplitude of the waves:

$$
\begin{aligned}
I_{s,p}(z) &= I_{s0,p0} - \frac{8 I_{s0} I_{p0}}{I_t} \gamma^{-1}(1 - 8\gamma^{-1}) \\
&\quad \times \sin^2\left\{ \frac{\Delta k z}{2}[1 + 4\gamma^{-1} - 8\gamma^{-2}(1 + \beta)] \right\} \\
&\quad + O(\gamma^{-3}),
\end{aligned}
\tag{A11}
$$

$$
\begin{aligned}
I_h(z) &= \frac{16 I_{s0} I_{p0}}{I_t} \gamma^{-1}(1 - 8\gamma^{-1}) \\
&\quad \times \sin^2\left\{ \frac{\Delta k z}{2}[1 + 4\gamma^{-1} - 8\gamma^{-2}(1 + \beta)] \right\} \\
&\quad + O(\gamma^{-3}),
\end{aligned}
\tag{A12}
$$

$$\phi_{s,p}(z) = \frac{\Delta k z}{2}[h_{s,p}^{(1)}\gamma^{-1} + h_{s,p}^{(2)}\gamma^{-2} + h_{s,p}^{(3)}\gamma^{-3} + h_{s,p}^{(4)}\gamma^{-4}] + O(\gamma^{-5}), \tag{A13}$$

where the $h_{s,p}^{(j)}$ functions are defined by the following relations:

$$h_{s,p}^{(1)} = -4N_{p0,s0}\frac{t_2(\phi)}{\phi},$$

$$h_{s,p}^{(2)} = -8\left[(\beta - 4N_{p0,s0})\frac{t_2(\phi)}{\phi} + 2N_{p0,s0}^2\frac{t_4(\phi)}{\phi}\right],$$

$$h_{s,p}^{(3)} = -32\left\{2[N_{p0,s0}(4+\beta) - 2\beta]\frac{t_2(\phi)}{\phi} + N_{p0,s0}(\beta - 8N_{p0,s0})\frac{t_4(\phi)}{\phi} + 2N_{p0,s0}^3\frac{t_6(\phi)}{\phi}\right\}. \tag{A14}$$

APPENDIX B: RESULTS OF HOMOGENIZATION

In the paper we apply several times a general homogenization theorem that we state and prove in this appendix. The small adimensional parameter δ is, in our framework, equal to $\gamma^{-1/2}$. We set $\tilde{E}_j = E_j/\sqrt{I_t}$ and $\tilde{z} = I_t z/(P_c \Delta k)$; the systems of Eqs. (11), (16), and (21) read, for Eq. (B3) below with $d = 6$, as

$$X^\varepsilon = [\mathrm{Re}(\tilde{E}_s), \mathrm{Im}(\tilde{E}_s), \mathrm{Re}(\tilde{E}_p), \mathrm{Im}(\tilde{E}_p), \mathrm{Re}(\tilde{E}_h), \mathrm{Im}(\tilde{E}_h)], \tag{B1}$$

$$\begin{aligned} F(X,\zeta) = \{&\sqrt{\omega_s/\omega_p}[-X_3X_5\sin(\zeta) - X_4X_6\sin(\zeta) - X_3X_6\cos(\zeta) \\ &+ X_4X_5\cos(\zeta)]\sqrt{\omega_s/\omega_p}[X_3X_5\cos(\zeta) + X_4X_6\cos(\zeta) - X_3X_6\sin(\zeta) \\ &+ X_4X_5\sin(\zeta)]\sqrt{\omega_p/\omega_s}[-X_1X_5\sin(\zeta) - X_2X_6\sin(\zeta) - X_1X_6\cos(\zeta) \\ &+ X_2X_5\cos(\zeta)]\sqrt{\omega_p/\omega_s}[X_1X_5\cos(\zeta) + X_2X_6\cos(\zeta) - X_1X_6\sin(\zeta) \\ &+ X_2X_5\sin(\zeta)]\omega_h/\sqrt{\omega_p\omega_s}[X_1X_3\sin(\zeta) - X_2X_4\sin(\zeta) - X_1X_4\cos(\zeta) \\ &- X_2X_3\cos(\zeta)]\omega_h/\sqrt{\omega_p\omega_s}[X_1X_3\cos(\zeta) - X_2X_4\cos(\zeta) + X_1X_4\sin(\zeta) \\ &+ X_2X_3\sin(\zeta)]\}. \end{aligned} \tag{B2}$$

Note that the theorem holds true only with real vector-valued functions, so we need to separate the real and the imaginary parts of our problems before applying the theorem.

Theorem. Let $(x,z) \in \mathbb{R}^d \times \mathbb{R}^+ \mapsto F(x,\zeta)$ be a periodic function with respect to the variable ζ with period Z_0 and $\int_0^{Z_0} F(x,\zeta)\mathrm{d}\zeta = 0$ for every $x \in \mathbb{R}^d$.

Let $X^\delta(z,t)$, taking values in $\mathbb{R}^d$, be the solution of

$$\frac{\partial X^\delta}{\partial z} = \frac{1}{\delta}F\left(X^\delta, \frac{z}{\delta^2}\right) + G\left(\frac{\partial X^\delta}{\partial t}, \frac{\partial^2 X^\delta}{\partial t^2}\right) \tag{B3}$$

starting from $X^\delta(t, z=0) = X_0(t)$. Then X^δ converges as $\delta \to 0$ to X, the solution of

$$\frac{\partial X}{\partial z} = b(X) + G\left(\frac{\partial X}{\partial t}, \frac{\partial^2 X}{\partial t^2}\right) \tag{B4}$$

starting from $X(t, z=0) = X_0(t)$, where

$$b_j(x) := -\sum_{i=1}^{d}\frac{1}{Z_0}\int_0^{Z_0}\mathrm{d}\zeta\int_0^{\zeta}\mathrm{d}\eta F_i(x,\zeta)\frac{\partial F_j}{\partial x_i}(x,\eta).$$

Demonstration. The proof is standard and is based on the so-called perturbed function method.[22] First we construct a slight perturbation of X^δ:

$$\bar{X}^\delta(z,t) = X^\delta(z,t) + \delta f_1\left[X^\delta(z,t), \frac{z}{\delta^2}\right] + \delta^2 f_2\left[X^\delta(z,t), \frac{z}{\delta^2}\right], \tag{B5}$$

$$f_1(x,\zeta) := -\int_0^{\zeta}F(x,\eta)\mathrm{d}\eta, \tag{B6}$$

$$f_2(x,\zeta) := -\int_0^{\zeta}[F(x,\eta)\nabla]f_1(x,\eta)\mathrm{d}\eta + \zeta b(x). \tag{B7}$$

Because the average value of F over a period is 0, the function f_1 is uniformly bounded. So is the function f_2 because the term $\zeta b(x)$ has been added so the increment of f_2 over a period is 0. By deriving $\bar{X}^\delta$ with respect to z we get

$$\begin{aligned} \frac{\partial \bar{X}^\delta(z,t)}{\partial z} = &\frac{1}{\delta}F\left(X^\delta, \frac{z}{\delta^2}\right) + \frac{1}{\delta}\frac{\partial f_1}{\partial \zeta}\left(X^\delta, \frac{z}{\delta^2}\right) \\ &+ F\left(X^\delta, \frac{z}{\delta^2}\right)\nabla_x f_1\left(X^\delta, \frac{z}{\delta^2}\right) + \frac{\partial f_2}{\partial \zeta}\left(X^\delta, \frac{z}{\delta^2}\right) \\ &+ G(X_t^\delta, X_{tt}^\delta) + O(\delta), \end{aligned}$$

where the first two terms on the right-hand side cancel by definition (B6) of f_1. The third and fourth terms partially cancel according to the definition (B7) of f_2, and only $b(X^\delta) + G(X_t^\delta, X_{tt}^\delta) + O(\delta)$ remains. By integrating from 0 to z and using the fact that $X^\delta(z) = \bar{X}^\delta(z) + O(\delta)$, we get

$$X^\delta(z,t) - X_0(t) = \int_0^z b[X^\delta(z',t)] + G[X_t^\delta(z',t), X_{tt}^\delta(z',t)]\mathrm{d}z' + O(\delta).$$

Letting $\delta \to 0$, we get the integral form of Eq. (B4), which completes the proof of the theorem.

ACKNOWLEDGMENTS

We thank A. Boscheron and C. Sauteret for useful and stimulating discussions. This study was performed un-

der the auspices of the Laser MegaJoule Program of Commissariat à l'Energie Atomique/Direction des Applications Militaires of France.

L. Videau's e-mail address is videau@bordeaux.cea.fr.

REFERENCES

1. M. Andre, "Megajoule solid state laser for ICF applications," in *Technical Committee Meeting on Drivers and Ignition Facilities for Inertial Fusion*, J. Coutant, ed., Proceedings of the International Atomic Energy Agency (Commissariat à l'Energie Atomique/Direction des Applications Militaires, Limeil-Valenton, France, 1995), pp. 77–78.
2. J. E. Rothenberg, "Comparison of beam-smoothing methods for direct-drive inertial confinement fusion," J. Opt. Soc. Am. B **14**, 1664–1671 (1997).
3. R. H. Lehmberg and S. P. Obenschain, "Use of induced spatial incoherency for uniform illumination," Opt. Commun. **46**, 27–31 (1983).
4. J. Garnier, L. Videau, C. Gouedard, and A. Migus, "Statistical analysis for beam smoothing and some applications," J. Opt. Soc. Am. A **14**, 1928–1937 (1997).
5. D. Veron, G. Thiell, and C. Gouedard, "Optical smoothing of the high power laser Phebus Nd-glass laser using the multimode optical fiber technique," Opt. Commun. **97**, 259–271 (1993).
6. J. E. Rothenberg, "Two-dimensional smoothing by spectral dispersion for direct-drive inertial confinement fusion," in *Solid State Lasers for Application to Inertial Confinement Fusion (ICF)*, W. F. Krupke, ed., Proc. SPIE **2633**, 634–644 (1995).
7. J. Garnier, J. P. Fouque, L. Videau, C. Gouédard, and A. Migus, "Amplification of broadband incoherent light in homogeneously broadened media in the presence of Kerr nonlinearity," J. Opt. Soc. Am. B **14**, 2563–2569 (1997).
8. G. Stegeman, M. Shiek-Bahae, E. Van Stryland, and G. Assanto, "Large nonlinear phase shifts in second-order nonlinear-optical processes," Opt. Lett. **18**, 13–15 (1993).
9. D. C. Hutchings, J. S. Aitchison, and C. N. Ironside, "All-optical switching based on nondegenerate phase shifts from a cascaded second-order nonlinearity," Opt. Lett. **18**, 793–795 (1993).
10. I. Buchvarov, S. Saltiel, Ch. Iglev, and K. Koynov, "Intensity dependent change of the polarization state as a result of non-linear phase shift in type II frequency doubling crystals," Opt. Commun. **141**, 173–179 (1997).
11. R. DeSalvo, D. J. Hagan, G. Stegeman, and E. W. Van Stryland, "Self-focusing and self-defocusing by cascaded second-order effects in KTP," Opt. Lett. **18**, 574–576 (1993).
12. A. E. Siegman, *Lasers* (University Science, Mill Valley, Calif., 1986).
13. D. Middleton, *Introduction to Statistical Communication Theory* (McGraw-Hill, New York, 1960).
14. J. T. Manassah, "Self-phase modulation of incoherent light revisited," Opt. Lett. **16**, 1439–1441 (1991).
15. J. W. Goodman, "Statistical properties of speckle patterns," in *Laser Speckle and Related Phenomena*, J. C. Dainty, ed., Vol. 9 of Topics in Applied Physics (Springer-Verlag, Berlin, 1984), pp. 9–75.
16. A. Yariv, *Quantum Electronics* (Wiley, New York, 1988).
17. J. T. Manassah, "Phase modulation in second-order nonlinear-optical processes," Phys. Rev. A **42**, 4085–4101 (1990).
18. A. C. L. Boscheron, "Etude de nouvelles configurations de conversion de frequence pour l'optimisation des lasers de haute puissance," Ph.D. dissertation (University of Paris XI, Orsay, France, 1996).
19. A. Kobyakov and F. Lederer, "Cascading of quadratic nonlinearities: an analytical study," Phys. Rev. A **54**, 3455–3471 (1996).
20. M. Abramowitz and I. Stegun, *Handbook of Mathematical Functions* (Dover, New York, 1970).
21. P. F. Byrd and M. D. Friedman, *Handbook of Elliptic Integrals for Engineers and Physicists* (Springer-Verlag, Berlin, 1954).
22. A. Bensoussan, J.-L. Lions, and G. Papanicolaou, *Asymptotic Analysis for Periodic Structures* (North-Holland, Amsterdam, 1978).